

Electronic Supplementary Information (ESI)

An Alternative Synthetic Approach for Macro-Meso-Microporous Metal–Organic Framework via “Domain Growth” Mechanism

Guowu Zhan and Hua Chun Zeng*

NUS Graduate School for Integrative Sciences and Engineering, and Department of Chemical and Biomolecular Engineering, Faculty of Engineering, National University of Singapore, 10 Kent Ridge Crescent, Singapore 119260

*Email: chezhc@nus.edu.sg

Table of Contents

ESI-1 Experimental methods	4
ESI-2 STEM characterization	6
ESI-3 FESEM characterization	7
ESI-4 XRD and UV–Vis diffuse reflectance characterizations.....	8
ESI-5 Digital photographs	9
ESI-6 FTIR characterization	10
ESI-7 XPS characterization	11
ESI-8 TGA characterization.....	12
ESI-9 Calcination treatments (in air or in Ar).....	13
ESI-10 The effect of PVP concentration	16
ESI-11 The effect of solvent (solvent polarity)	18
ESI-12 The effect of reaction temperature	21
ESI-13 Scale-up experiments	22
ESI-14 Nitrogen physisorption characterization	23
ESI-15 Comparative experiments	24
ESI-16 Characterizations of Cu ₂ O nanocubes	25
ESI-17 Other characterization of HKUST-1 3D-nets.....	26
ESI-18 Dye adsorption performance of the HKUST-1	28
ESI-19 Oxidative cyclization reaction using HKUST-1 as catalysts	30
References.....	31

Supplementary Figures

Figure S1. (a-i) High-angle annular dark-field scanning TEM (HAADF-STEM) images (at different magnifications) of the as-prepared HKUST-1 3D-nets.	6
Figure S2. Representative FESEM images (at different magnifications) of the as-synthesized HKUST-1 3D-nets.	7
Figure S3. XRD patterns of the as-synthesized HKUST-1 3D-nets (prepared by using Cu ₂ O nanocubes providing copper ion source) and the HKUST-1 octahedrons (prepared by using CuCl ₂ salt providing copper ion source, refer to the experimental method in SI-1).	8
Figure S4. UV–Vis diffuse reflectance spectra of HKUST-1 materials in 3D-nets shape (prepared by using Cu ₂ O nanocubes providing copper ion source) and octahedron shape (prepared by using CuCl ₂ salt providing copper ion source, refer to the experimental method in SI-1).	8
Figure S5. Digital photographs and TEM images of as-synthesized HKUST-1 3D-nets and HKUST-1 octahedrons in the as-made mother liquors.	9
Figure S6. Digital photograph of the as-synthesized HKUST-1 octahedrons after drying (60°C for 12 h).	9
Figure S7. FTIR spectrum of the as-prepared HKUST-1 3D-nets.	10
Figure S8. Deconvoluted Cu 2 <i>p</i> , C 1 <i>s</i> , O 1 <i>s</i> , and N 1 <i>s</i> XPS spectra of HKUST-1 3D-nets.	11
Figure S9. Thermogravimetric analysis curves for HKUST-1 3D-nets under air (red curve) or nitrogen (black curve) atmospheres.	12
Figure S10. (a-f) Typical TEM images (at different magnifications) of the CuO nanoparticles prepared by calcination treatments of HKUST-1 3D-nets at 280°C in static air for 6 h (heating rate at 2°C/min). Inset in (f): size distribution of the CuO nanoparticles.	13
Figure S11. XRD pattern of the product prepared by calcination treatments of HKUST-1 3D-nets at 280°C in static air for 6 h (heating rate at 2°C/min).	13
Figure S12. (a-f) Typical TEM images (at different magnifications) of the Cu/carbon hybrids prepared by calcination treatments of HKUST-1 3D-nets at 400°C in an Ar flow (50 mL/min) for 2 h (heating rate at 2°C/min). (g) XRD patterns of the products.	14
Figure S13. (a-i) Typical TEM images (at different magnifications) and (j) XPS C 1 <i>s</i> spectrum of the amorphous carbon prepared by firstly calcination treatments of HKUST-1 3D-nets at 400°C in an Ar flow (50 mL/min) for 2 h (heating rate at 2°C/min), then washing with nitric acid (14.5 mol/L).	15
Figure S14. Digital photograph of as-synthesized product by adding a large amount of PVP (5 times of the normal amount, Experimental condition C1).	16
Figure S15. (a-c) Typical TEM images (at different magnifications) of the HKUST-1 product prepared by without adding PVP (Experimental condition C2).	17
Figure S16. (a-f) Typical TEM images (at different magnifications) of the HKUST-1 product prepared from Experimental condition C3.	18
Figure S17. (a-f) TEM images (at different magnifications) of the HKUST-1 product prepared from Experimental condition C4.	19
Figure S18. (a-f) TEM images (at different magnifications) of the HKUST-1 product	

prepared from Experimental condition C5.....	20
Figure S19. (a-f) TEM images (at different magnifications) of the HKUST-1 3D-nets prepared from at room temperature (Experimental condition C6).....	21
Figure S20. XRD patterns of the HKUST-1 products prepared under different reaction temperature. R.T. represents “room temperature”.....	21
Figure S21. (a-d) TEM images (at different magnifications) of the HKUST-1 3D-nets in a scale-up experiment (Experimental condition C7).....	22
Figure S22. BJH pore size distribution of HKUST-1 3D-nets calculated from the N ₂ desorption branch of the isotherms shown in the main text. Note that a logarithm scale is used for the <i>x</i> -axis.	23
Figure S23. (a-f) Typical TEM images (at different magnifications) of the HKUST-1 octahedral crystals prepared from Condition C8.....	24
Figure S24. Typical TEM images (at different magnifications) of the products prepared by using (a,b) Cu(NO ₃) ₂ , (c,d) CuBr, (e,f) Cu(OAc) ₂ , and (g,h) CuSO ₄ as copper ion sources.....	24
Figure S25. (a-d) Typical TEM images (at different magnifications) of the Cu ₂ O nanocubes with an average edge side of 60 nm.	25
Figure S26. Selected area electron diffraction (SAED) pattern and high resolution TEM (HRTEM) of a Cu ₂ O nanocube with the electron beam parallel to the [001] direction. .	25
Figure S27. (a-f) High-resolution TEM images of the HKUST-1 3D-nets.	26
Figure S28. Time evolution of product morphology of the reaction system examined by TEM.	27
Figure S29. The chemical structure of methylene blue (MB).	28
Figure S30. UV-vis spectra of methylene blue (MB) solutions as a function of time with HKUST-1 3D-nets as an adsorbent (a) or HKUST-1 octahedrons as an adsorbent (b)...	28
Figure S31. Plots of pseudo-second-order kinetics of MB adsorption over HKUST-1 3D-nets (a) and HKUST-1 octahedrons (b). The unit for <i>k</i> is g/(mg·min).	29
Figure S32. The oxidative cyclization reaction between 2-hydroxyacetophenone and phenylenediamine.	30
Figure S33. GC-MS spectra from a reaction mixture after the oxidative cyclization reaction by using HKUST-1 3D-nets as a catalyst (refer to Experimental Section).	30
Figure S34. XRD patterns of HKUST-1 3D-net samples after catalysis reaction and dye adsorption experiments.	31

Supplementary Table

Table S1. Textural properties of the synthesized HKUST-1 with different morphologies.....	23
--	----

ESI-1 Experimental methods

Materials. The following chemicals were used as received without further purification: copper (II) chloride dihydrate (Sigma-Aldrich, >99%), copper (II) nitrate trihydrate (Sigma-Aldrich, 99-104%), copper (II) acetate monohydrate (Sigma-Aldrich, >99%), copper (II) sulfate pentahydrate (Nacalai Tesque, 99.5%), copper (I) bromide (Aldrich, 99.99%), 1,3,5-benzenetricarboxylic acid (H_3BTC , 95%, Aldrich), polyvinylpyrrolidone (PVP, Aldrich, K-30), L-Ascorbic acid (Sigma-Aldrich, 99%), sodium hydroxide (Merck, 99%), 2-hydroxyacetophenone (Aldrich, 98%), o-phenylenediamine (Aldrich, 99.5%), n-dodecane (Alfa Aesar, 99%), methylene blue (MB, Merck), N,N'-dimethylformamide (DMF, Merck, 99.8%), benzyl alcohol (Aldrich, 99%), toluene (J.T.Baker, 99.5%), and ethanol (Fisher, 99.99%). Deionized water was used for all experiments.

Synthesis of Cu_2O nanocubes. Specifically, 0.1 mmole of $CuCl_2$ and 0.1 g of PVP were dissolved in 40 mL of water, followed by a dropwise addition (30 $\mu L/s$) of 2.5 mL of aqueous NaOH (0.20 M). Then, the solution was stirred magnetically for 5 min, followed by a dropwise addition (10 $\mu L/s$) of 2.5 mL of aqueous ascorbic acid (0.10 M). After the addition, the mixture was further stirred for 5 min. The product was recovered by centrifugation and then washed with ethanol twice. Finally, the yellow colored Cu_2O nanocubes were re-dispersed into 10 mL of ethanol for the future use. Note that all the reactions were carried out at room temperature (25°C).

Synthesis of HKUST-1 3D-nets. Firstly, 0.5 mL of ethanolic H_3BTC solution (0.1 M), 0.5 mL of DMF and 0.1 mL of PVP (10 g/L, ethanolic solution) were mixed with 1 mL of the prepared Cu_2O ethanolic suspension. Afterwards, the reaction was carried out at room temperature for 3 h or at 80°C for 1 h. The product was collected by centrifugation and washing with ethanol twice.

Synthesis of HKUST-1 by using metal salts as copper ion source. 0.5 mL of ethanolic H_3BTC solution (0.10 M) was mixed with 0.5 mL of DMF and 0.1 mL of PVP (10 g/L, ethanolic solution). Then, 0.01 mmole of $CuCl_2$ or $Cu(NO_3)_2$ or $Cu(OAc)_2$ or $CuBr_2$ or $CuSO_4$ (dissolved in 1 mL of ethanol) was added under mild stirring. Then the reaction was carried out at 80°C for 1 h. The product was collected by centrifugation and washing with ethanol twice.

Oxidative cyclization reaction.¹ Typically, 20 mg of HKUST-1 catalysts were dispersed in 10 mL of toluene by sonication for 15 min. Then, the suspension was mixed with a mixture of containing 2-hydroxyacetophenone (0.136 g, 1.0 mmole), phenylenediamine (0.119 g, 1.1 mmole), n-dodecane (0.1 mL, as internal standard), and toluene (10 mL). The reaction mixture was stirred at 100°C under the oxygen bubbling (30 mL/min). The products after removing the catalysts and quenching with ethyl acetate were analyzed by gas chromatograph (GC, Agilent 7890A) and GC-mass spectrometry (GC: HP 6890 and mass selective detector: HP 5973). The conversion was calculated based on 2-hydroxyacetophenone.

Dye adsorption experiments. The adsorption capacities of HKUST-1 samples were investigated by mixing MB aqueous solutions (50 mL, 50 ppm) with 12 mg of HKUST-1 solid under neutral

conditions at room temperature. The dye solutions containing the HKUST-1 were mixed well with magnetic stirring and maintained for a fixed time. After adsorption for a pre-determined time, the solution was separated from the adsorbents by centrifugation (6000 rpm, 3min) and the solutions were measured by using UV-visible absorption spectroscopy. The dye concentration was determined by measuring the absorbance at $\lambda = 664$ nm (*i.e.*, maximum absorbance for MB). It should be noted that the dried samples of HKUST-1 3D-nets were in film state, so they were grounded into powder with carnelian mortar before the mixing with dye solution.

Characterization techniques. Morphologies of samples were characterized by field-emission scanning electron microscopy (FESEM, JSM-6700F), transmission electron microscopy (TEM, JEM-2010), and high-angle annular dark-field scanning TEM (HAADF-STEM, JEM-2100F). The crystallographic information was analyzed by X-ray diffraction (XRD, Bruker D8 Advance) equipped with a Cu K_α radiation source. The elemental mapping was done by energy-dispersive X-ray (EDX, Oxford Instruments, Model 7426). The surface composition and oxidation state of the samples were further analyzed by X-ray photoelectron spectroscopy (XPS, AXIS-HSi, Kratos Analytical). Specific surface areas, pore volume, and pore size of the samples were determined using N_2 physisorption isotherms at 77 K (Quantachrome NOVA-3000 system). Thermogravimetric analysis (TGA) studies were carried out on a thermobalance (TGA-2050, TA Instruments) under flowing air or N_2 atmosphere (flow rate: 50 mL/min) at a heating rate of 10°C/min. The organic groups in the HKUST-1 structures were characterized by Fourier transform infrared spectroscopy (FTIR, Bio-Rad). UV-Vis diffuse reflectance spectra were collected using a Shimadzu 3600 UV-VIS-NIR spectrophotometer equipped with an integrating sphere in the 190–2000 nm range ($BaSO_4$ was used as a white standard).

ESI-2 STEM characterization

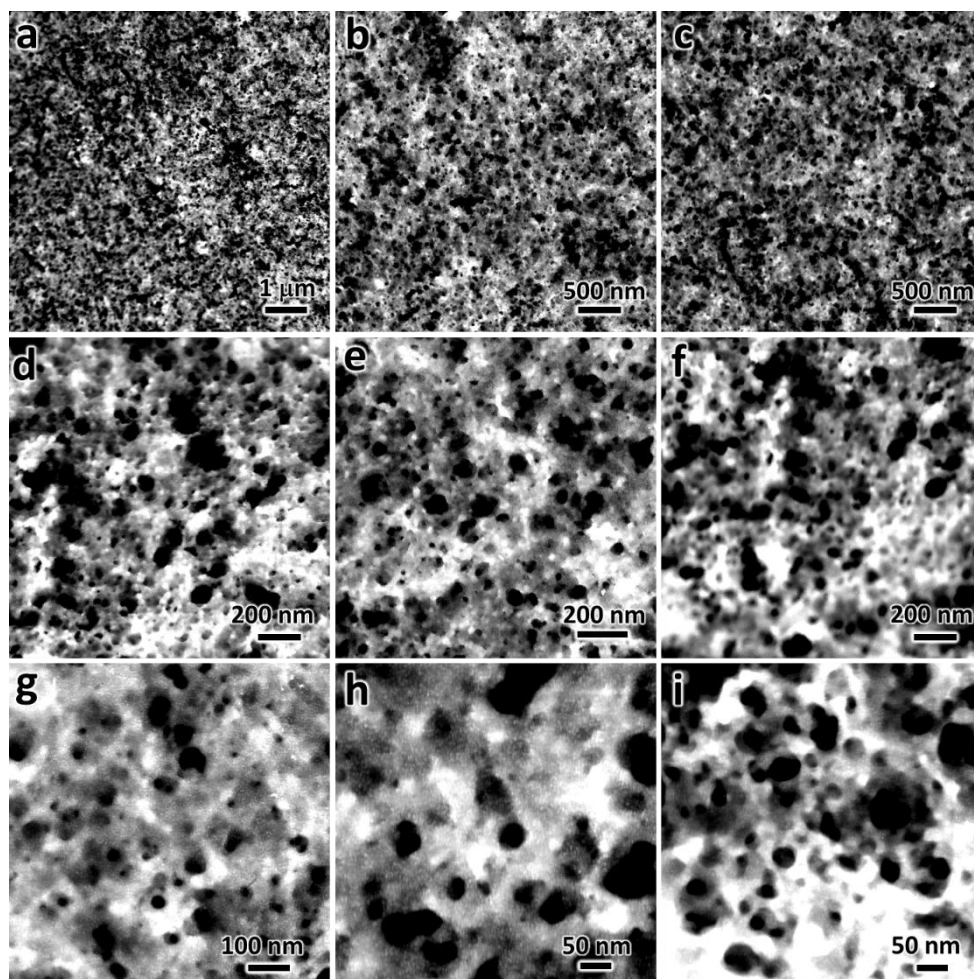


Figure S1. (a-i) High-angle annular dark-field scanning TEM (HAADF-STEM) images (at different magnifications) of the as-prepared HKUST-1 3D-nets.

ESI-3 FESEM characterization

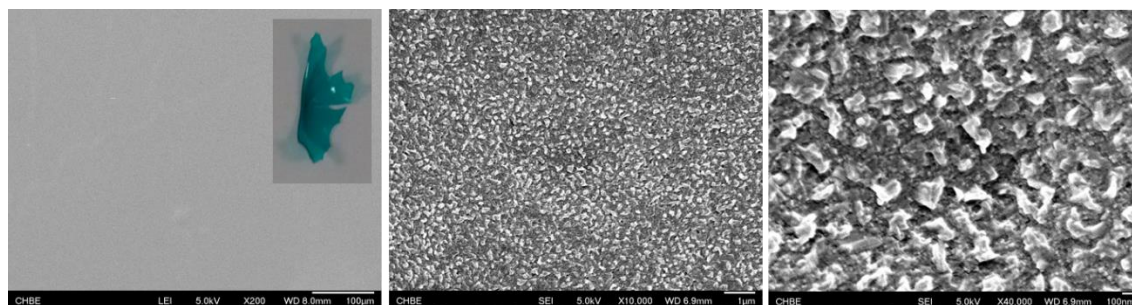


Figure S2. Representative FESEM images (at different magnifications) of the as-synthesized HKUST-1 3D-nets.

Comments: The sample for FESEM observation was collected from a small piece of the dry film (shown in the inset).

ESI-4 XRD and UV–Vis diffuse reflectance characterizations

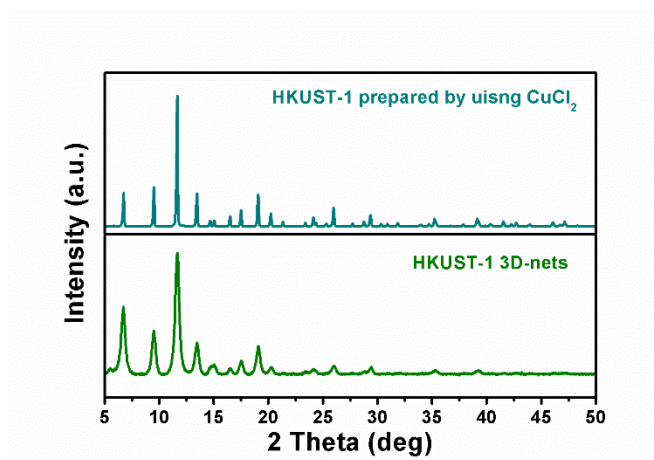


Figure S3. XRD patterns of the as-synthesized HKUST-1 3D-nets (prepared by using Cu₂O nanocubes providing copper ion source) and the HKUST-1 octahedrons (prepared by using CuCl₂ salt providing copper ion source, refer to the experimental method in SI-1).

Comments: From the comparison of the two patterns, it can be concluded that the HKUST-1 products prepared from these two different methods show the identical crystallinity. The peak broadening observed in the 3D-nets is because the crystallites in the spongy HKUST-1 are nanosized (*ca.* 20 nm).

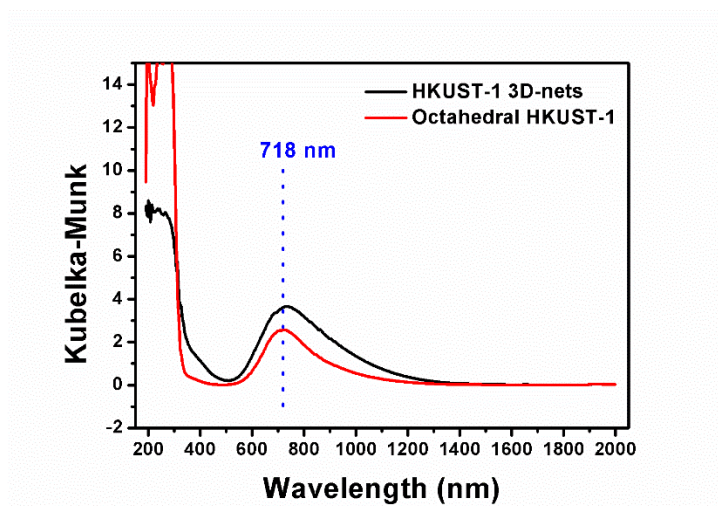


Figure S4. UV–Vis diffuse reflectance spectra of HKUST-1 materials in 3D-nets shape (prepared by using Cu₂O nanocubes providing copper ion source) and octahedron shape (prepared by using CuCl₂ salt providing copper ion source, refer to the experimental method in SI-1).

ESI-5 Digital photographs

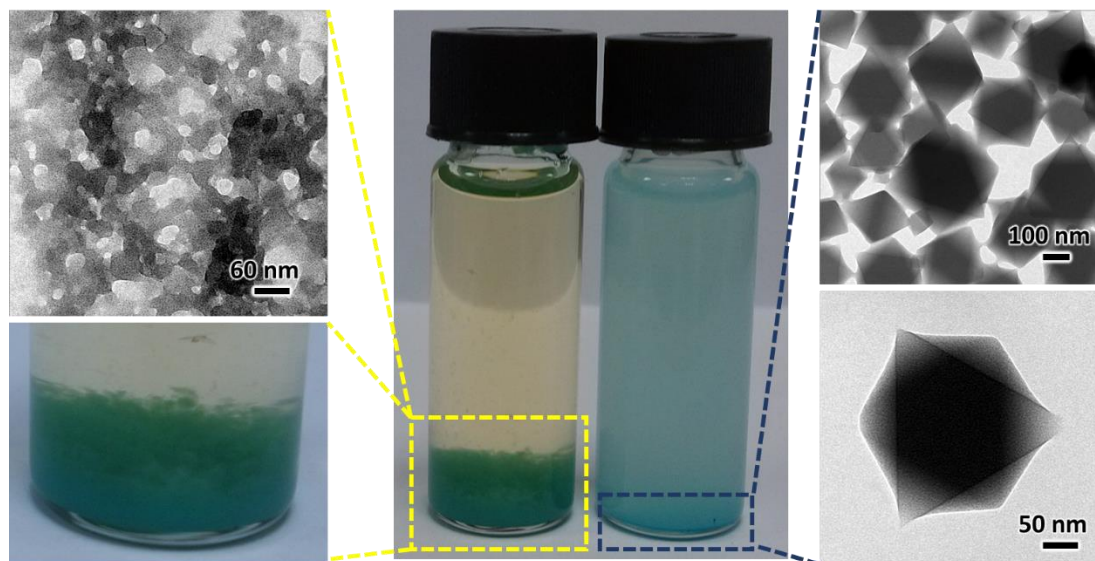


Figure S5. Digital photographs and TEM images of as-synthesized HKUST-1 3D-nets and HKUST-1 octahedrons in the as-made mother liquors.

Comments: The results indicate the difference in the apparent bulk density caused by sizes and shapes of the nanostructures.



Figure S6. Digital photograph of the as-synthesized HKUST-1 octahedrons after drying (60°C for 12 h).

ESI-6 FTIR characterization

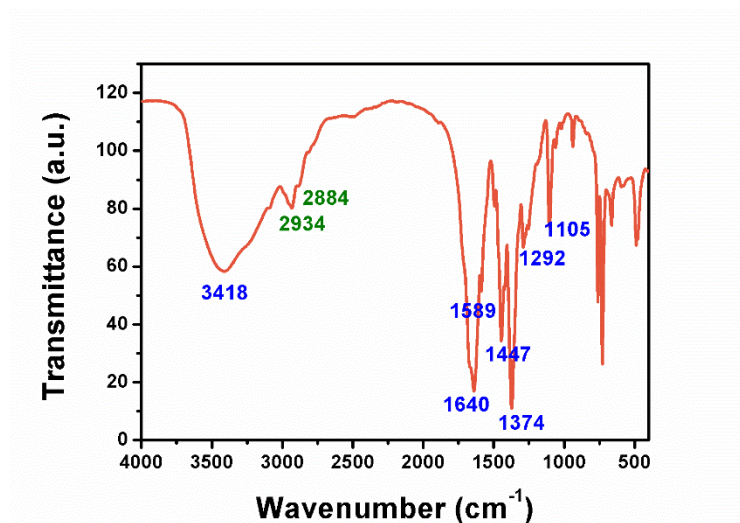


Figure S7. FTIR spectrum of the as-prepared HKUST-1 3D-nets.

Comments: The FTIR spectrum of HKUST-1 3D-nets looks rather similar to the reported data of HKUST-1 prepared from conventional hydrothermal method.² The main characteristics peaks belong to the carboxylate groups in BTC³⁻, and the in-plane or out-of-plane vibrations of the C–H groups in benzene ring.³ In addition, the characteristic bands at 2934 and 2884 cm⁻¹ (C–H stretch) are indicative the presence of residual DMF solvent or PVP in the HKUST-1 3D-nets.⁴ But the intensities of these two bands are relatively low, suggesting the little amount of the residual DMF solvent or PVP.

ESI-7 XPS characterization

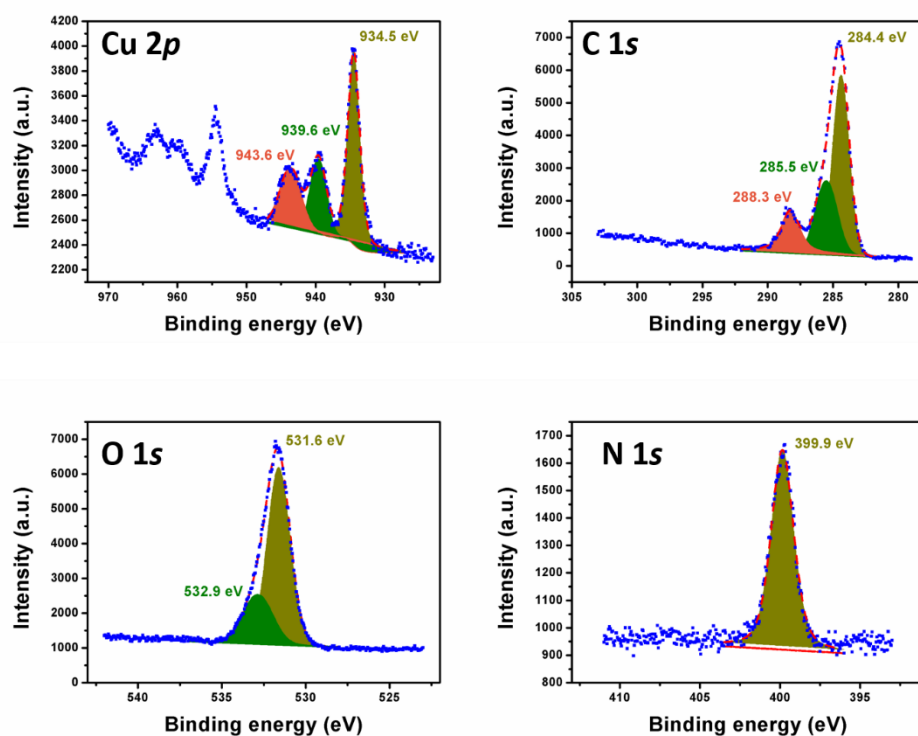


Figure S8. Deconvoluted Cu 2p, C 1s, O 1s, and N 1s XPS spectra of HKUST-1 3D-nets.

Comments: The nitrogen signal was originated from the residual PVP molecules on the HKUST-1 solid. The quantitative analysis of the elements on the surface is shown in the following table.

	Cu 2p	O 1s	C 1s	N 1s
Atomic concentration %	2.47	18.83	75.51	3.19
Mass concentration%	11.11	21.37	64.34	3.17

ESI-8 TGA characterization

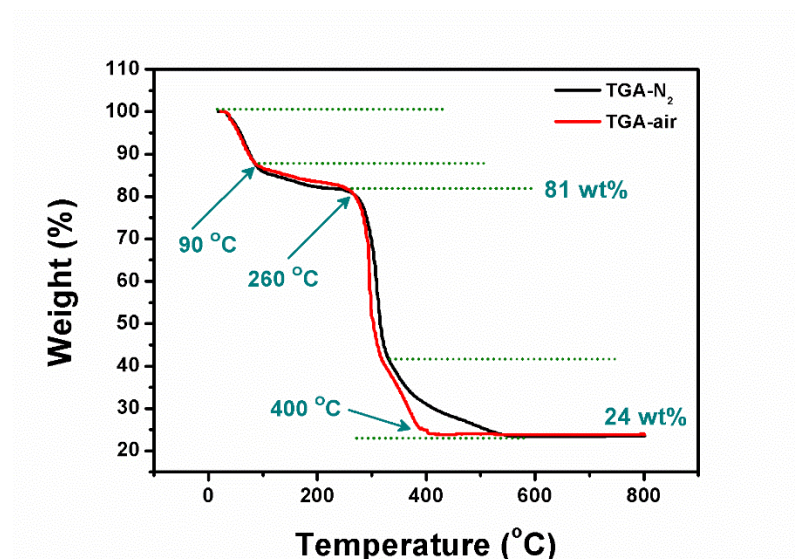


Figure S9. Thermogravimetric analysis curves for HKUST-1 3D-nets under air (red curve) or nitrogen (black curve) atmospheres.

Comments: The TGA curves exhibit several steps of weight losses. The first two weight losses (between 20–90°C and 90–260°C) correspond to the removal of moisture (7.5 wt%) and captured DMF molecules (11.5 wt%). After that, a sharp decomposition occurred at 260 to 400°C can be ascribed to the thermal decomposition of both the organic ligands and a few amount of residual PVP molecules.⁵ Beyond 400°C, there is no weight change (in air) with increasing temperature. Due to that the decomposition temperature of PVP is similar to the organic ligand (BTC³⁻) in HKUST-1, TGA result was not able to determine the PVP content. The copper content in product was 28.2% (as measured by ICP), which is slightly different from the calculated data from the molecular formula Cu₃(BTC)₂ (31.5 wt%). So, we believe that the maximum impurity content in HKUST-1 is 10 wt%, but the actual PVP amount should be much lower than this value due to the impurities in sample for ICP test may contain moisture or remained DMF.

ESI-9 Calcination treatments (in air or in Ar)

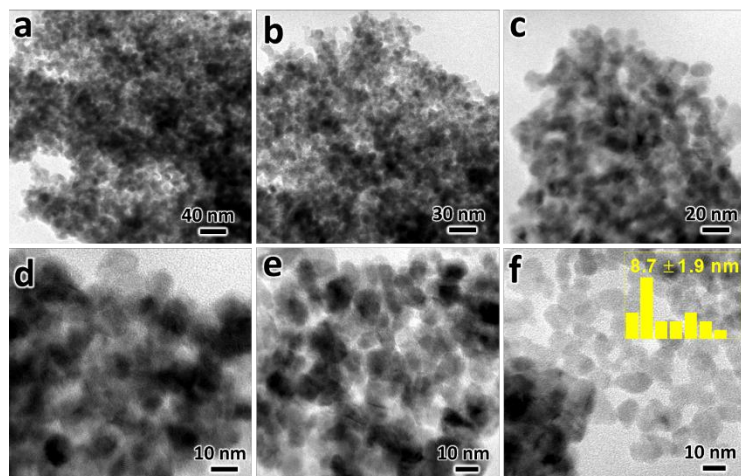


Figure S10. (a-f) Typical TEM images (at different magnifications) of the CuO nanoparticles prepared by calcination treatments of HKUST-1 3D-nets at 280°C in static air for 6 h (heating rate at 2°C/min). Inset in (f): size distribution of the CuO nanoparticles.

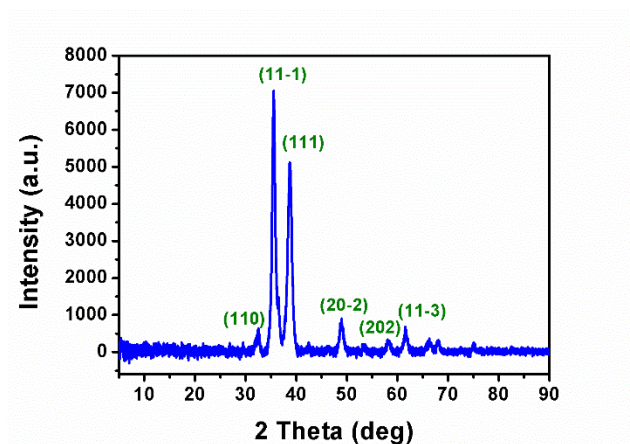


Figure S11. XRD pattern of the product prepared by calcination treatments of HKUST-1 3D-nets at 280°C in static air for 6 h (heating rate at 2°C/min).

Comments: As shown, the product can be assigned to phase pure CuO (JCPDS card no. 48-1548).

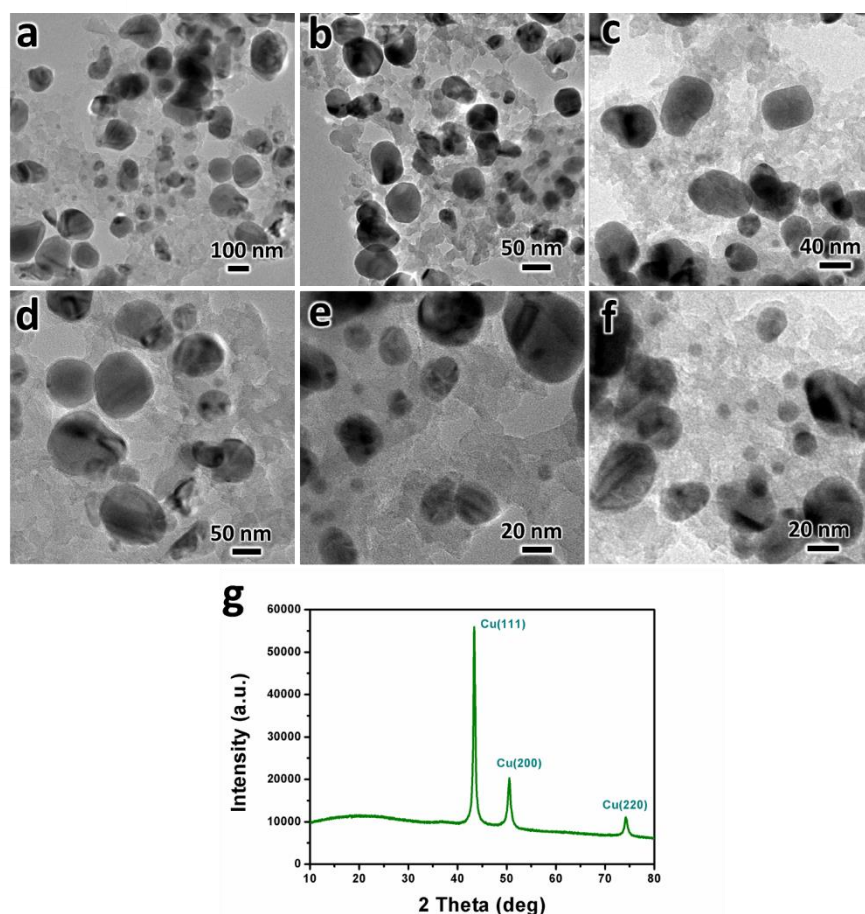


Figure S12. (a-f) Typical TEM images (at different magnifications) of the Cu/carbon hybrids prepared by calcination treatments of HKUST-1 3D-nets at 400°C in an Ar flow (50 mL/min) for 2 h (heating rate at 2°C/min). (g) XRD patterns of the products.

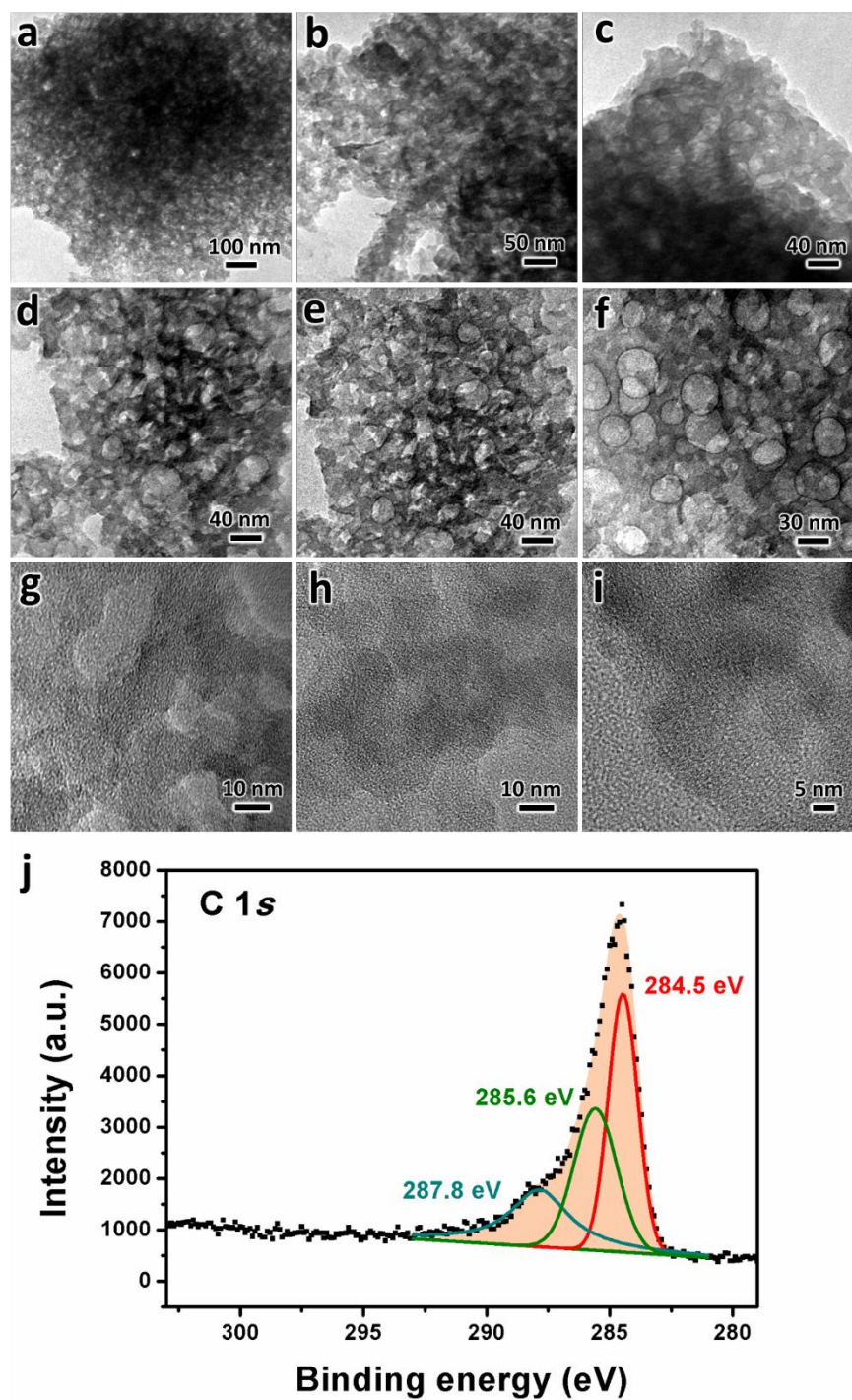


Figure S13. (a-i) Typical TEM images (at different magnifications) and (j) XPS C 1s spectrum of the amorphous carbon prepared by firstly calcination treatments of HKUST-1 3D-nets at 400°C in an Ar flow (50 mL/min) for 2 h (heating rate at 2°C/min), then washing with nitric acid (14.5 mol/L).

ESI-10 The effect of PVP concentration

Two comparison experiments were carried out to investigate the effect of PVP concentration: (1) in the absence of PVP, (2) with the addition of higher amounts of PVP (five times of the standard amount).

Experimental condition C1 (large amount of PVP). Firstly, 0.5 mL of ethanolic H_3BTC solution (0.1 M) was mixed with 0.5 mL of DMF and 0.5 mL of PVP (10 g/L, ethanolic solution, 5 times of the normal amount). Then, 1 mL of Cu_2O ethanolic suspension was added under mild stirring. The reaction was carried out at 80°C for 16 h.

Comments: Under this condition, we found that no solid product can be obtained (even collection by centrifugation, see the photo below), although the reaction was proceeded at 80°C for 16 h. Firstly, the color of the solution changed from yellow to green and no yellow colored solid (Cu_2O) left, which means the total decomposition and oxidation of Cu_2O to Cu^{2+} ions. It is inferred that large amount of PVP would inhibit the crystallization of the HKUST-1, probably by the strong interaction between copper ions and the PVP molecules (the pyrrolidone rings ($\text{C}=\text{O}$)).



Figure S14. Digital photograph of as-synthesized product by adding a large amount of PVP (5 times of the normal amount, Experimental condition C1).

Experimental condition C2 (without the addition of PVP). Firstly, 0.5 mL of ethanolic H₃BTC solution (0.1 M) was mixed with 0.5 mL of DMF and 0.1 mL of ethanol (no PVP was dissolved within the ethanol). Then, 1 mL of Cu₂O ethanolic suspension was added under mild stirring. The reaction was carried out at 80°C for 1 h. Finally, the product was collected by centrifugation and washing with ethanol twice. The TEM images of the resulting product are shown below.

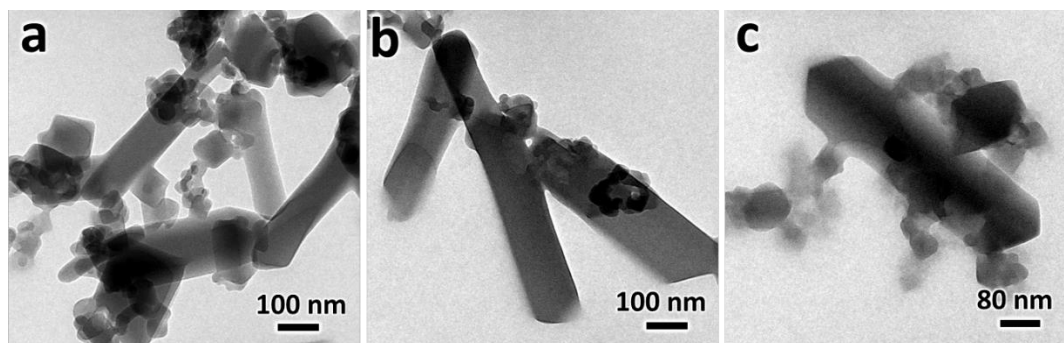


Figure S15. (a-c) Typical TEM images (at different magnifications) of the HKUST-1 product prepared by without adding PVP (Experimental condition C2).

Comments: As shown, the products are aggregates with indefinite shapes and a broad size distribution. HKUST-1 3D-nets were not found in this case (without the addition of PVP). This experiment also indicates that PVP is a critical additive for the formation of HKUST-1 3D-nets.

ESI-11 The effect of solvent (solvent polarity)

Experimental condition C3 (using large amount of DMF). Firstly, 0.5 mL of ethanolic H₃BTC solution (0.1 M) was mixed with 1.5 mL of DMF and 0.1 mL of PVP (10 g/L, ethanolic solution). Then, 1 mL of Cu₂O ethanolic suspension was added under mild stirring. The reaction was carried out at 80°C for 1 h. Finally, the product was collected by centrifugation and washing with ethanol twice. The TEM images of the resulting product are shown below.

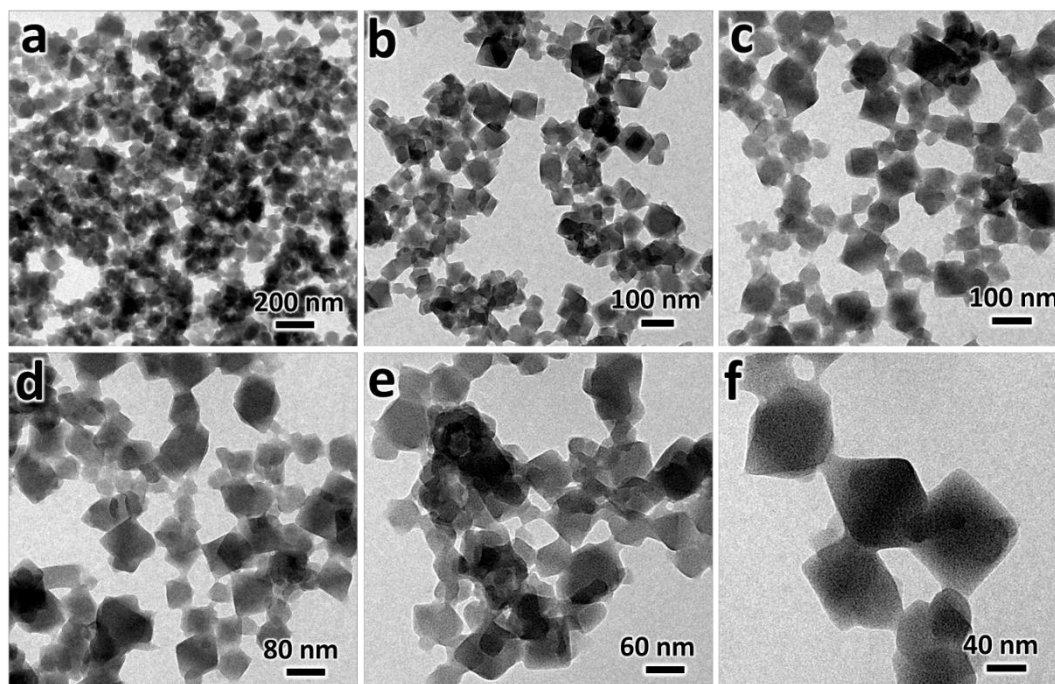


Figure S16. (a-f) Typical TEM images (at different magnifications) of the HKUST-1 product prepared from Experimental condition C3.

Comments: A large amount of high-polar solvent (*viz.*, DMF with dielectric constant of 36.7) can promote the dissociation of organic ligand molecules and the decomposition of Cu₂O nanocubes, then enhance the coordination rate between copper ions and the organic ligands. We also observed that in this case, the time required for color change of the solution from yellow to blue was much shorter than other experiments. Therefore, under this condition, only discrete HKUST-1 particles were prepared instead of the 3D-nets.

Experimental condition C4 (without using DMF). Firstly, 0.5 mL of ethanolic H₃BTC solution (0.1 M) was mixed with 0.5 mL of ethanol and 0.1 mL of PVP (10 g/L, ethanolic solution). Then, 1 mL of Cu₂O ethanolic suspension was added under mild stirring. The reaction was carried out at 80°C for 1 h. Finally, the product was collected by centrifugation and washing with ethanol twice. The TEM images of the resulting product are shown below.

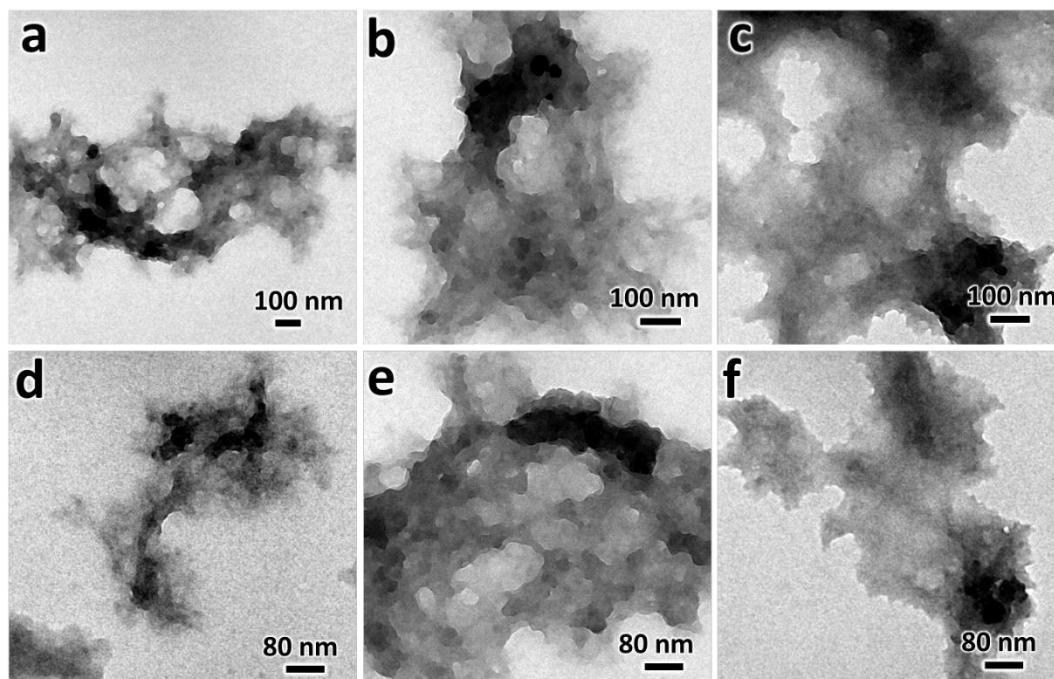


Figure S17. (a-f) TEM images (at different magnifications) of the HKUST-1 product prepared from Experimental condition C4.

Comments: We found that the shape of product is very spongy without adding DMF. However, the networks were not integrated well, as they are in the forms of small pieces of HKUST-1. Apparently, from these TEM images, we can also find that the mesopores/macropores in the product are less than the normal HKUST-1 3D-nets.

Experimental condition C5 (using benzyl alcohol). Firstly, 0.05 mmole of H_3BTC was dissolved in 0.95 mL of benzyl alcohol and 0.05 mL of ethanol. Then, the H_3BTC solution was mixed with 0.1 mL of PVP (10 g/L, ethanolic solution). Afterward, 1 mL of Cu_2O ethanolic suspension was added under mild stirring. Then the reaction was carried out at 80°C for 1 h. Finally, the product was collected by centrifugation and washing with ethanol twice. The TEM images of the resulting product are shown below.

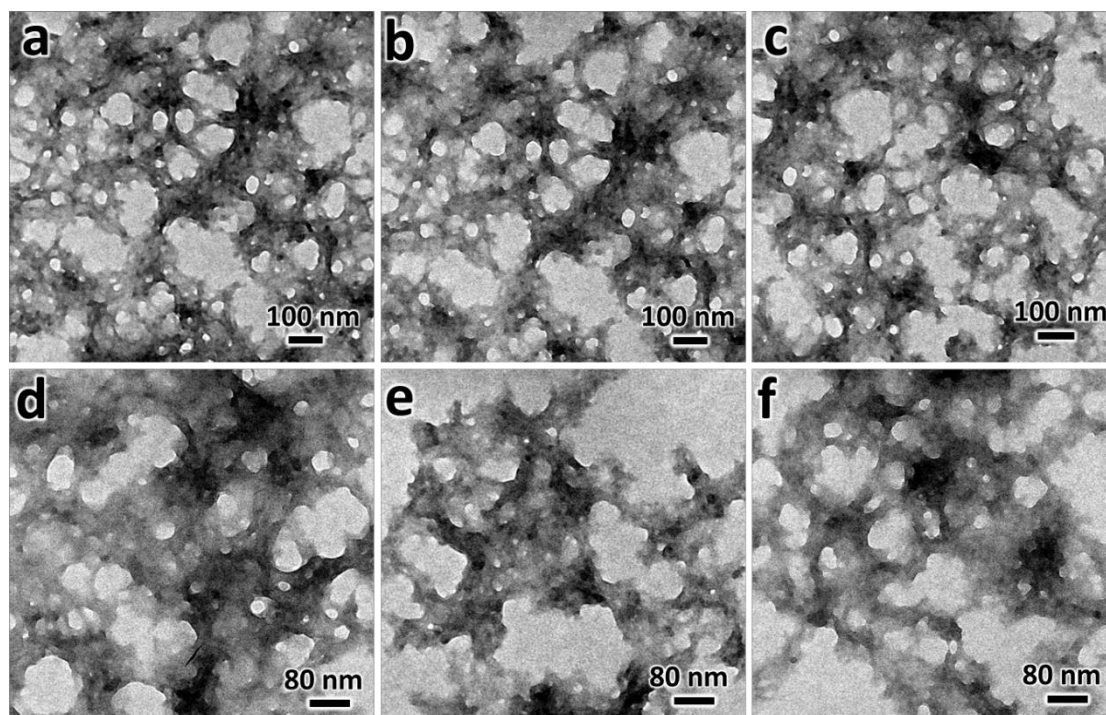


Figure S18. (a-f) TEM images (at different magnifications) of the HKUST-1 product prepared from Experimental condition C5.

Comments: We found that the use of a less polar solvent, benzyl alcohol (dielectric constant = 13), can still lead to the formation of HKUST-1 3D-nets. But the overall morphology of the HKUST-1 is slightly different from the one shown in the main text.

ESI-12 The effect of reaction temperature

Experimental condition C6 (reaction at room temperature). Firstly, 0.5 mL of ethanolic H_3BTC solution (0.1 M) was mixed with 0.5 mL of DMF and 0.1 mL of PVP (10 g/L, ethanolic solution). Then, 1 mL of Cu_2O ethanolic suspension was added under mild stirring. The reaction was carried out at room temperature for 3 h. Finally, the product was collected by centrifugation and washing with ethanol twice. The TEM images of the resulting product are shown below.

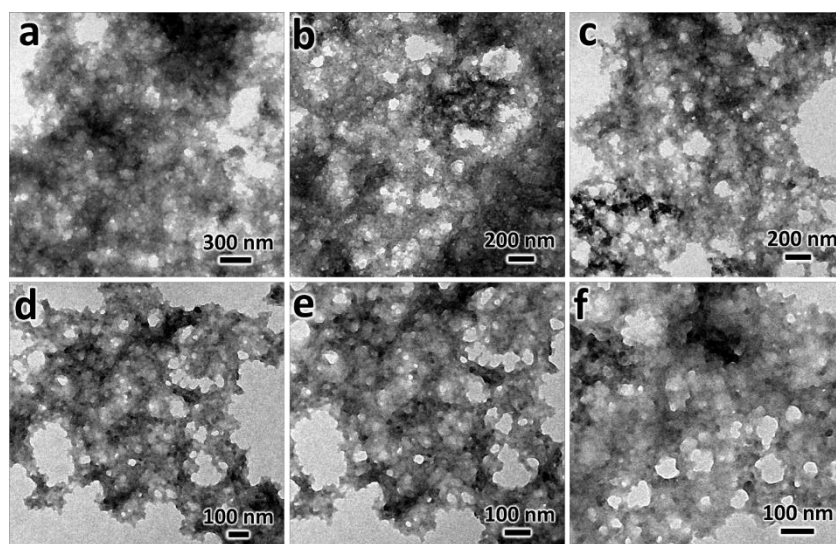


Figure S19. (a-f) TEM images (at different magnifications) of the HKUST-1 3D-nets prepared from at room temperature (Experimental condition C6).

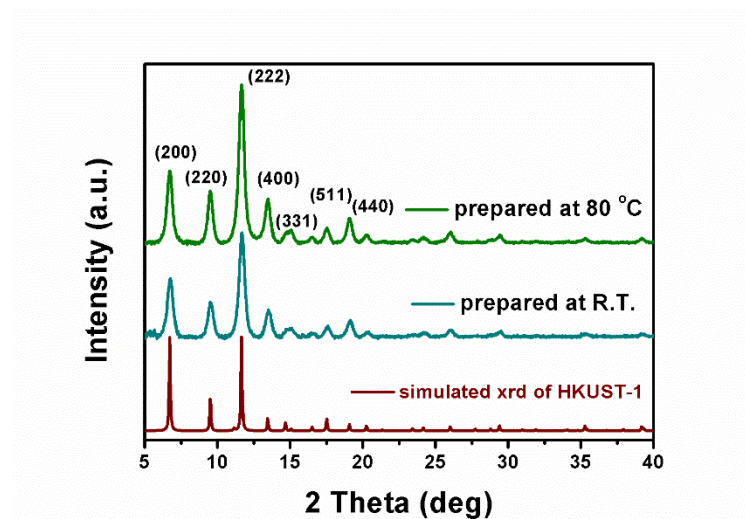


Figure S20. XRD patterns of the HKUST-1 products prepared under different reaction temperature. R.T. represents “room temperature”.

Comments: This experiment show that the reaction temperature is not a crucial factor for the growth of HKUST-1 in 3D-nets shapes. Moreover, we found that the reaction temperature will not affect the quality of products significantly, although more intense diffraction peaks are found in the sample prepared at 80°C.

ESI-13 Scale-up experiments

Experimental condition C7 (scale-up experiment). For the large scale experiment, the original total volume of reaction solution (2.1 mL) was changed to a total volume of 210 mL while maintain the same concentrations of each reagent. Specifically, 50 mL of ethanolic H_3BTC solution (0.1 M) was mixed with 50 mL of DMF and 10 mL of PVP (10 g/L, ethanolic solution). Then, 100 mL of Cu_2O ethanolic suspension was added under mild stirring. Then the reaction was carried out at 80°C for 1 h.

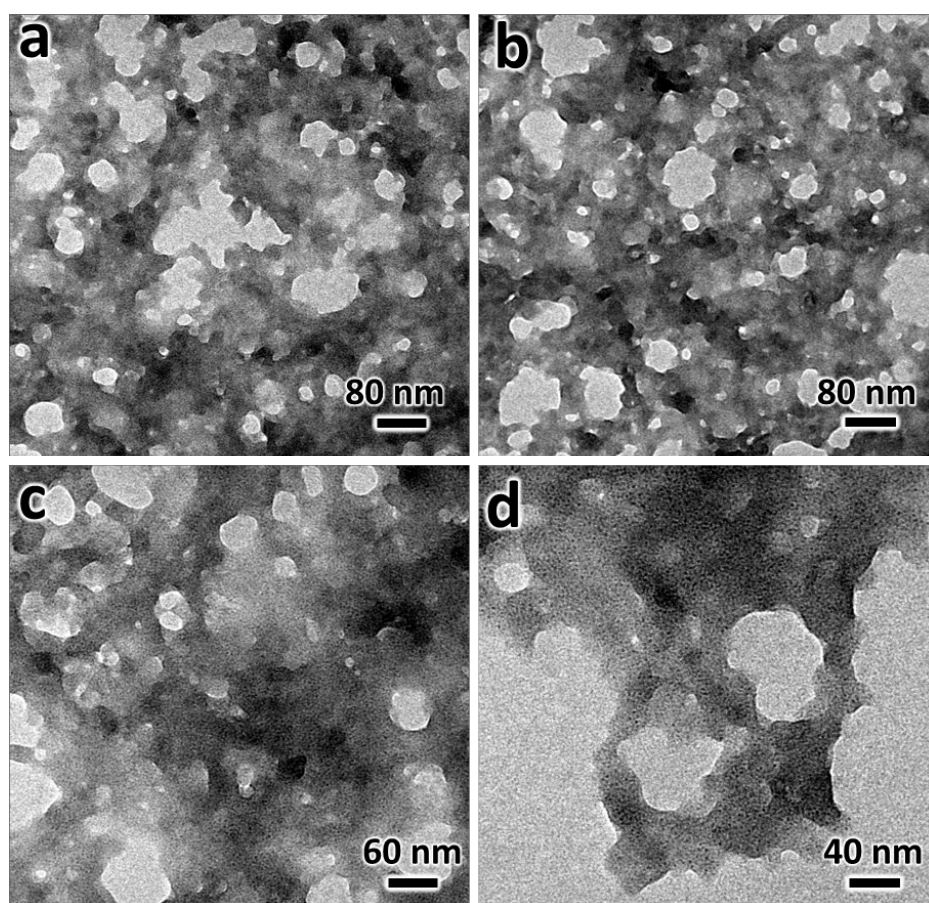


Figure S21. (a-d) TEM images (at different magnifications) of the HKUST-1 3D-nets in a scale-up experiment (Experimental condition C7).

Comments: As shown, similar product was obtained from the scale-up experiments, suggesting that the synthetic method is facile and scalable.

ESI-14 Nitrogen physisorption characterization

Table S1. Textural properties of the synthesized HKUST-1 with different morphologies.

Sample	S_{BET} (m^2/g)	S_{micro} (m^2/g)	S_{meso} (m^2/g)	$S_{\text{meso}}/S_{\text{micro}}$	V_{t} (cm^3/g)	V_{micro} (cm^3/g)	V_{meso} (cm^3/g)	$V_{\text{meso}}/V_{\text{micro}}$
3D-nets	680	430	250	0.58	0.46	0.17	0.29	1.7
Octahedrons	1060	910	150	0.16	0.42	0.37	0.05	0.14

Notes: S_{micro} is the t-plot-specific micropore surface area calculated from the N_2 isotherm. V_{t} is the total specific pore volume determined by using the adsorption branch of the N_2 isotherm at the highest P/P_0 (0.995). V_{micro} is the specific micropore volume calculated by subtracting V_{meso} from V_{t} , and V_{meso} is the specific mesopore volume obtained from the BJH calculation method.

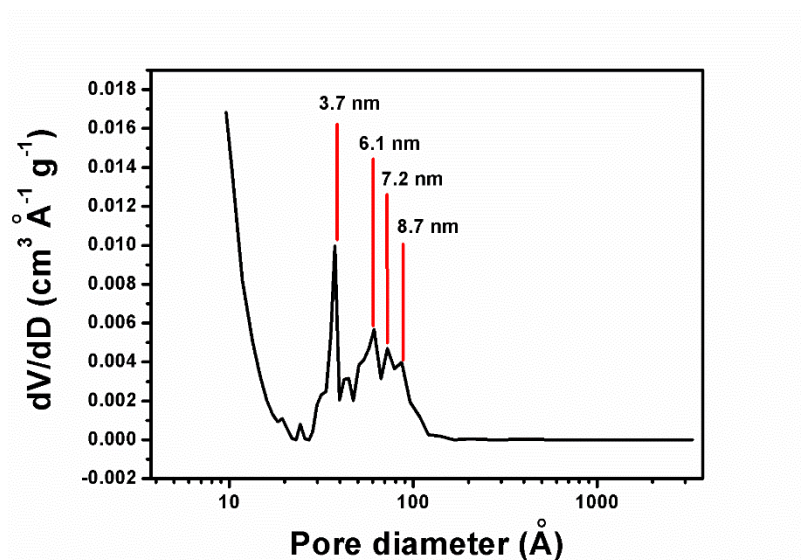


Figure S22. BJH pore size distribution of HKUST-1 3D-nets calculated from the N_2 desorption branch of the isotherm shown in the main text. Note that a logarithm scale is used for the x -axis.

ESI-15 Comparative experiments

Condition C8 (using CuCl_2 as copper ion source). Firstly, 0.5 mL of ethanolic H_3BTC solution (0.1 M) was mixed with 0.5 mL of DMF and 0.1 mL of PVP (10 g/L, ethanolic solution). Then, 0.01 mmole of CuCl_2 (dissolved in 1 mL of ethanol) was added under mild stirring. The reaction was carried out at 80°C for 1 h. Finally, the product was collected by centrifugation and washing with ethanol twice. The TEM images of the resulting products are shown below.

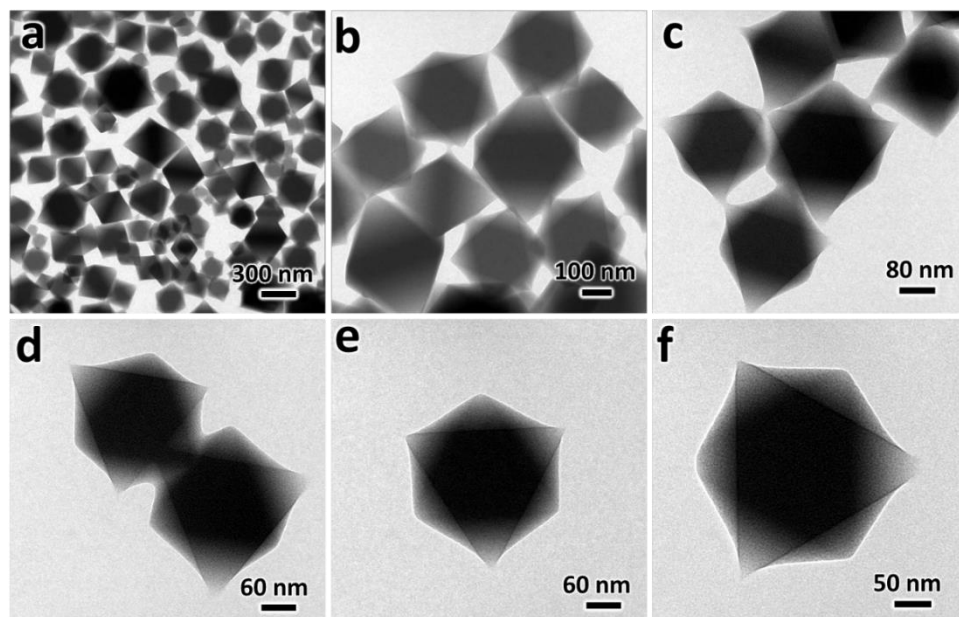


Figure S23. (a-f) Typical TEM images (at different magnifications) of the HKUST-1 octahedral crystals prepared from Condition C8.

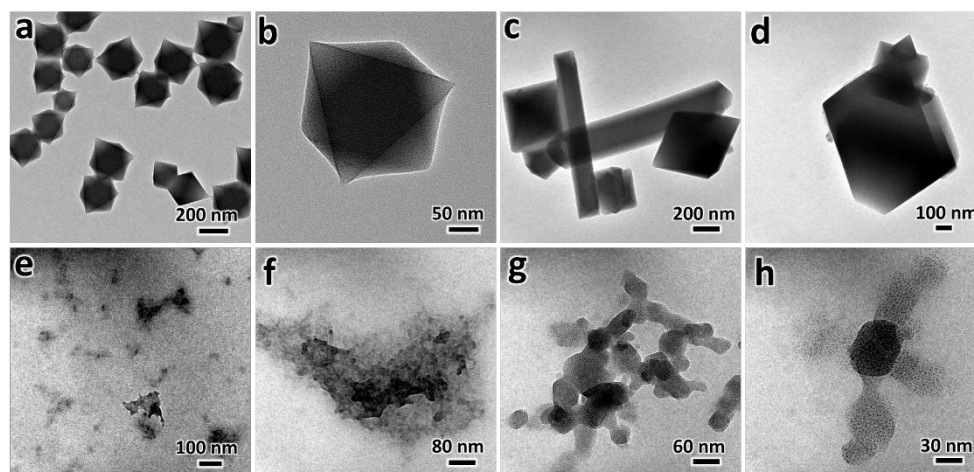


Figure S24. Typical TEM images (at different magnifications) of the products prepared by using (a,b) $\text{Cu}(\text{NO}_3)_2$, (c,d) CuBr , (e,f) $\text{Cu}(\text{OAc})_2$, and (g,h) CuSO_4 as copper ion sources.

ESI-16 Characterizations of Cu₂O nanocubes

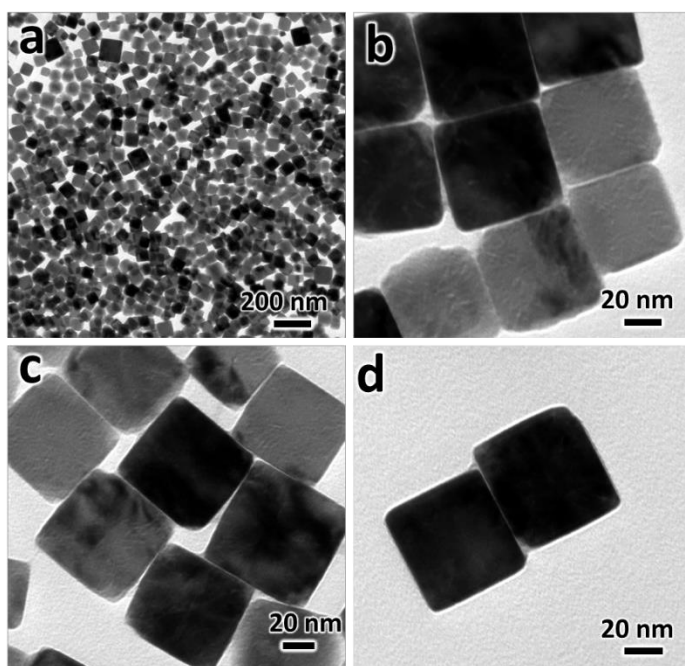


Figure S25. (a-d) Typical TEM images (at different magnifications) of the Cu₂O nanocubes with an average edge side of 60 nm.

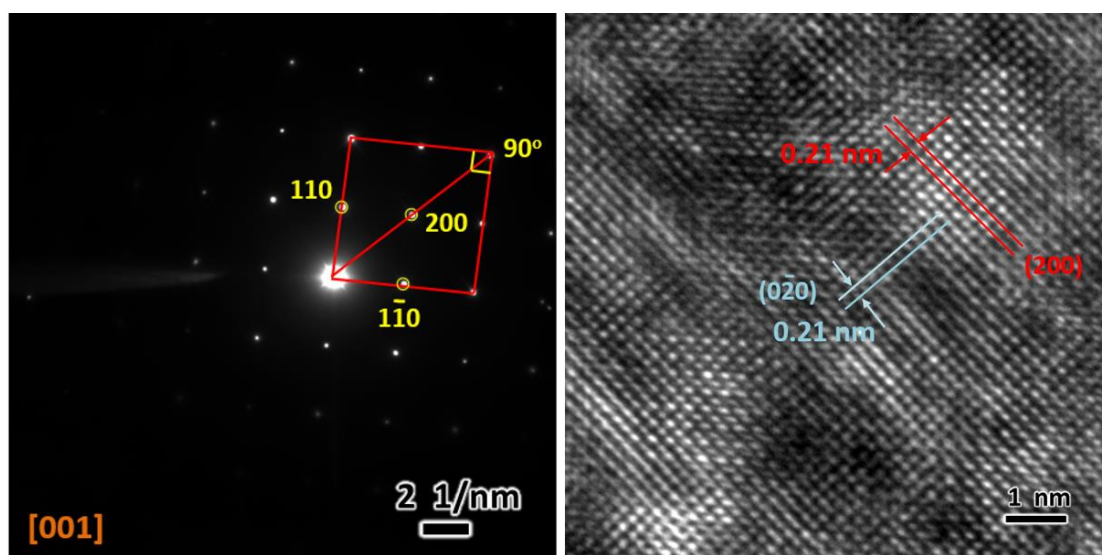


Figure S26. Selected area electron diffraction (SAED) pattern and high resolution TEM (HRTEM) of a Cu₂O nanocube with the electron beam parallel to the [001] direction.

Comments: As shown in the SAED, the spots ([001] zone) with a square symmetry indicate that the as-prepared nanocubes are single crystals exposed with the {100} facets.⁶

ESI-17 Other characterization of HKUST-1 3D-nets

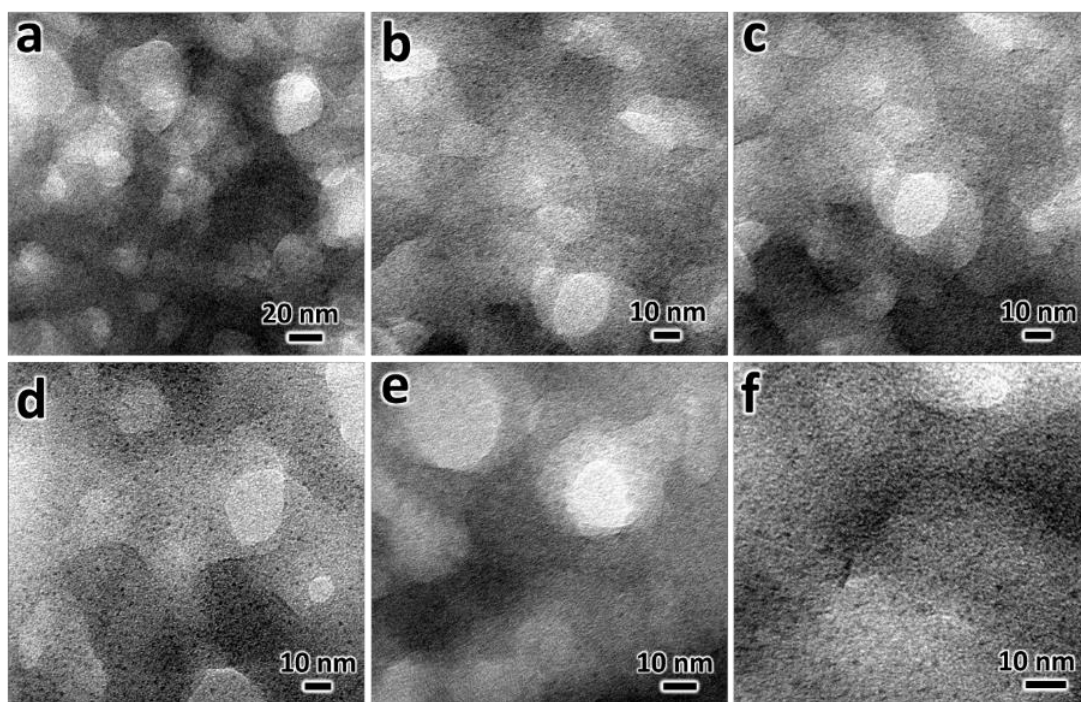


Figure S27. (a-f) High-resolution TEM images of the HKUST-1 3D-nets.

Comments: It should be noted that it was very difficult to get the lattice belonging to HKUST-1 because the samples were highly sensitive to the electron beam (the Cu^{2+} ions can even be reduced by the electrons!).

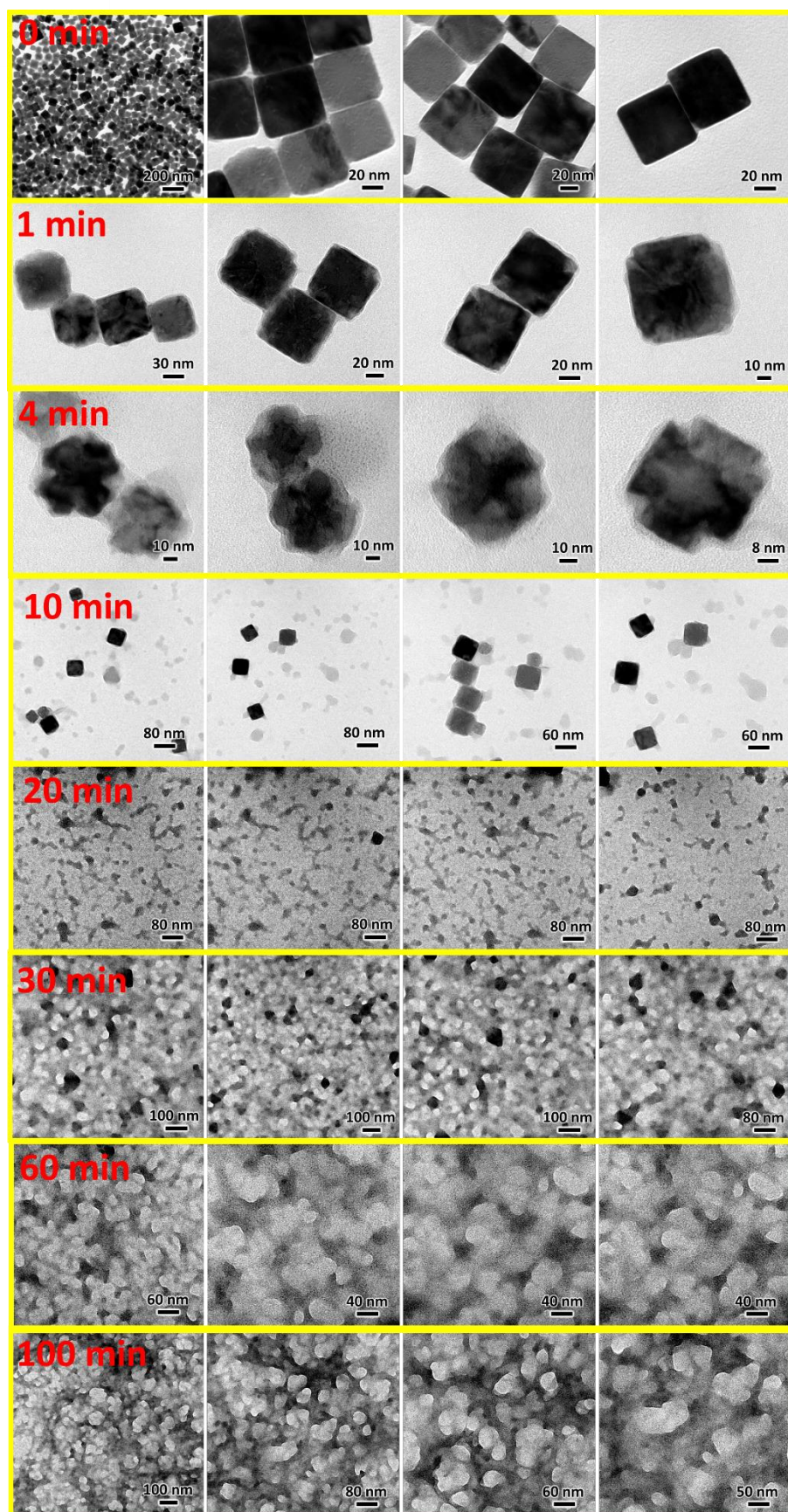


Figure S28. Time evolution of product morphology of the reaction system examined by TEM.

ESI-18 Dye adsorption performance of the HKUST-1

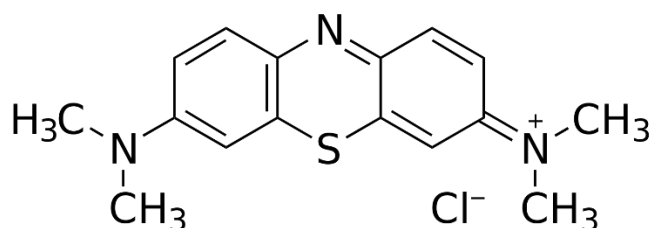


Figure S29. The chemical structure of methylene blue (MB).

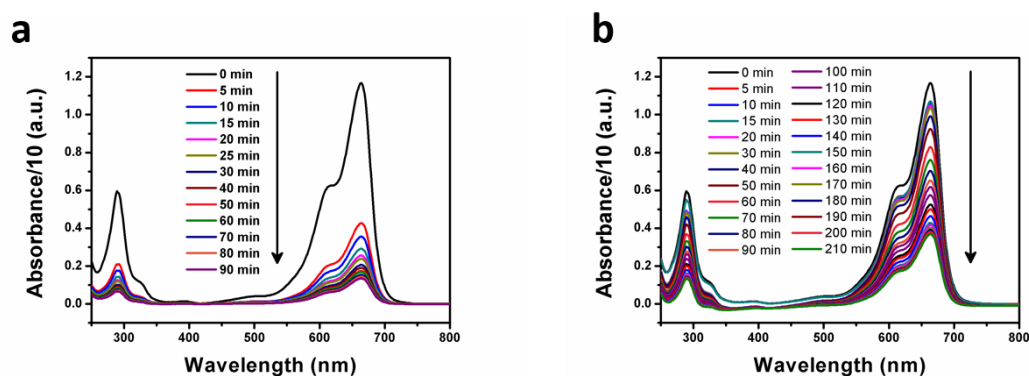


Figure S30. UV-vis spectra of methylene blue (MB) solutions as a function of time with HKUST-1 3D-nets as an adsorbent (a) or HKUST-1 octahedrons as an adsorbent (b).

The changes of adsorbed amount of MB with time can be fitted by using a pseudo-second-order kinetic model:⁷

$$\frac{dQ}{dt} = k(Q_0 - Q_t)^2$$

$$\frac{t}{Q_t} = \frac{1}{k * Q_0^2} + \frac{1}{Q_0} t$$

Where, Q_0 : amount adsorbed at equilibrium (mg/g), which can be derived from the slope of the fitting line (not from the experimental maximum data shown in the main text); Q_t : amount adsorbed at time t (mg/g); t : adsorption time (min); k : the second order kinetic constant.

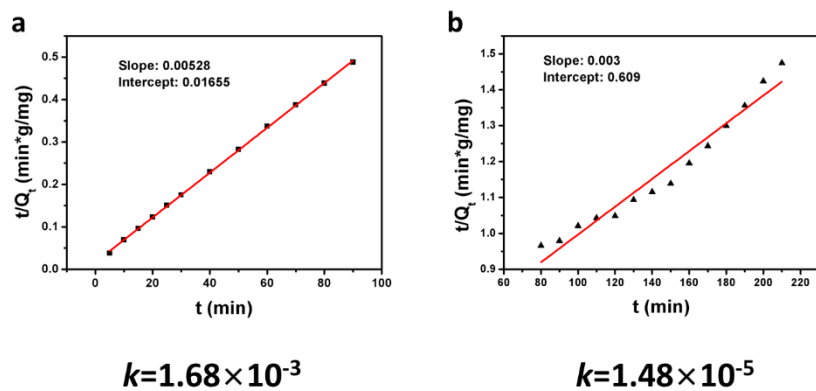


Figure S31. Plots of pseudo-second-order kinetics of MB adsorption over HKUST-1 3D-nets (a) and HKUST-1 octahedrons (b). The unit for k is $\text{g}/(\text{mg} \cdot \text{min})$.

ESI-19 Oxidative cyclization reaction using HKUST-1 as catalysts

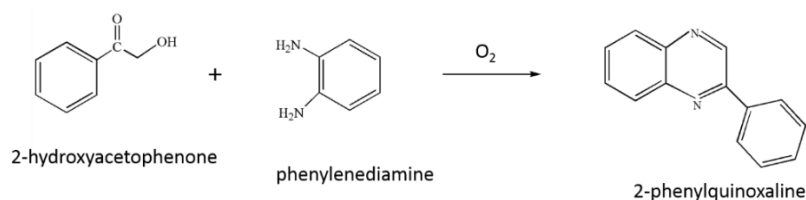


Figure S32. The oxidative cyclization reaction between 2-hydroxyacetophenone and phenylenediamine.

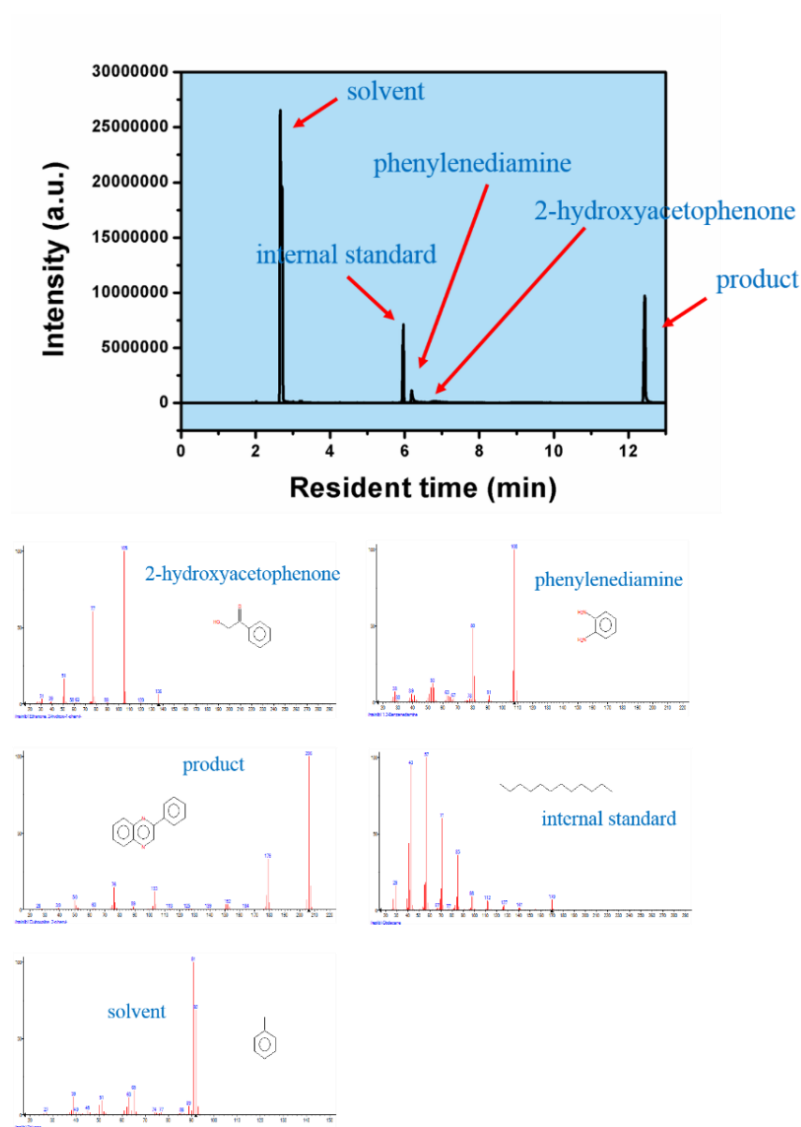


Figure S33. GC-MS spectra from a reaction mixture after the oxidative cyclization reaction by using HKUST-1 3D-nets as a catalyst (refer to Experimental Section).

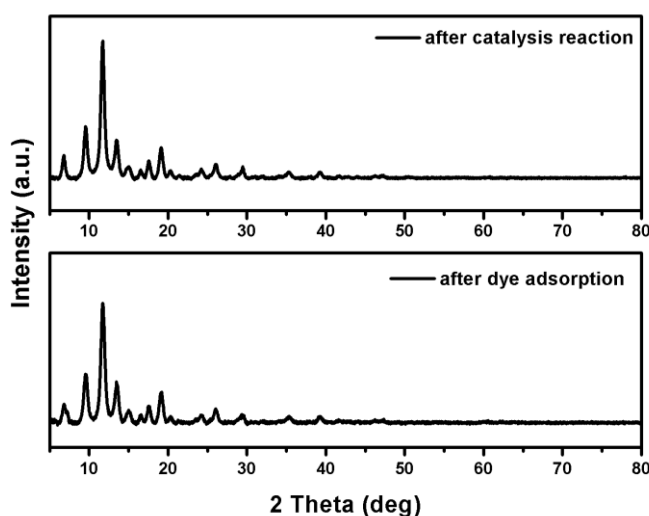


Figure S34. XRD patterns of HKUST-1 3D-net samples after catalysis reaction and dye adsorption experiments.

References

- (1) Dang, G. H.; Vu, Y. T. H.; Dong, Q. A.; Le, D. T.; Truong, T.; Phan, N. T. S. Quinoxaline synthesis via oxidative cyclization reaction using metal–organic framework Cu(BDC) as an efficient heterogeneous catalyst. *Applied Catalysis A: General* **2015**, *491*, 189.
- (2) Li, L.; Liu, X. L.; Geng, H. Y.; Hu, B.; Song, G. W.; Xu, Z. S. A MOF/graphite oxide hybrid (MOF: HKUST-1) material for the adsorption of methylene blue from aqueous solution. *Journal of Materials Chemistry A* **2013**, *1*, 10292.
- (3) Bordiga, S.; Lamberti, C.; Ricchiardi, G.; Regli, L.; Bonino, F.; Damin, A.; Lillerud, K. P.; Bjorgen, M.; Zecchina, A. Electronic and vibrational properties of a MOF-5 metal-organic framework: ZnO quantum dot behaviour. *Chemical Communications* **2004**, 2300.
- (4) Sethia, S.; Squillante, E. Solid dispersion of carbamazepine in PVP K30 by conventional solvent evaporation and supercritical methods. *International Journal of Pharmaceutics* **2004**, *272*, 1.
- (5) Peniche, C.; Zaldívar, D.; Pazos, M.; Páz, S.; Bulay, A.; Román, J. S. Study of the thermal degradation of poly(N-vinyl-2-pyrrolidone) by thermogravimetry–FTIR. *Journal of Applied Polymer Science* **1993**, *50*, 485.
- (6) Kim, M. H.; Lim, B.; Lee, E. P.; Xia, Y. Polyol synthesis of Cu₂O nanoparticles: use of chloride to promote the formation of a cubic morphology. *Journal of Materials Chemistry* **2008**, *18*, 4069.
- (7) Haque, E.; Jun, J. W.; Jung, S. H. Adsorptive removal of methyl orange and methylene blue from aqueous solution with a metal-organic framework material, iron terephthalate (MOF-235). *Journal of Hazardous Materials* **2011**, *185*, 507.